3D Mapping of Indoor Parking Space Using Edge Consistency Census Transform Stereo Odometry

Junesuk Lee and Soon-Yong Park[a]
School of Electronic and Electrical Engineering, Kyungpook National University, Daegu, South Korea

Keywords: 3D Mapping, 3D Reconstruction, 3D Scanning, Visual Odometry, Parking Ramp, Parking Space.

Abstract: In this paper, we propose a real-time 3D mapping system for indoor parking ramps and spaces. Visual odometry is calculated by applying the proposed Edge Consistency Census Transform (ECCT) stereo matching method. ECCT works strongly in repeated patterns and reduces drift errors in the vertical direction of the ground caused by Kanade-Lucas-Tomasi stereo matching of VINS-FUSION algorithm. We propose a mobile mapping system that uses a stereo camera and 2D lidar for data set acquisition. The parking ramp and spaces dataset are obtained using the mobile mapping system and are reconstructed using the proposed system. The proposed system performs the 3D mapping of the parking ramp and spaces dataset that is obtained using the mobile mapping system. We present the error of the normal vector with respect to the ground of the parking space as a quantitative evaluation for performance comparison with the previous method. Also, we present 3D mapping results as qualitative results.

1 INTRODUCTION

With the rapid development of technologies related to autonomous driving, the 3D mapping technology of real space is being actively researched. Self-driving cars use the HD map built in advance to safely drive in urban and highway environments, estimate the location of the car, plan the driving route, and safely drive to the destination (Kim et al., 2021; Ding et al., 2021). To create an HD map, the vehicle is combined with the camera, lidar, IMU, and GPS sensor to scan the surrounding environment. Such a device is called Mobile Mapping System (MMS) (Roh et al., 2016). In addition, the HD map is provided information such as traffic lights, traffic signs, and lanes that can affect the localization and path planning of autonomous vehicles (Elhousni et al., 2020). Considering the complete driving of the autonomous vehicle, the vehicle must be driven from the parked location to the parking spaces of the destination. Autonomous valet parking research (Qin et al., 2020; Chirca et al., 2015) aims to park a vehicle at a certain spot in the parking spaces. In addition to these studies, the problem of entering the parking space inside the building from the outdoor environment should be considered. In most cases of underground or above-ground parking included inside a building, it is necessary to pass through the parking ramp. In general, it is difficult to perform localization in the computer vision field because the parking ramp section has few textures and similar structures. Especially, in the case of a parking ramp in a building, if the width is narrow and the illumination is low, sit is difficult for autonomous vehicles to enter. Therefore, as one method for safe driving on the parking ramp, there is providing information on the width, height, length, curvature, and slope of the ramp section. In the International Building Code (International Code Council, 2018),

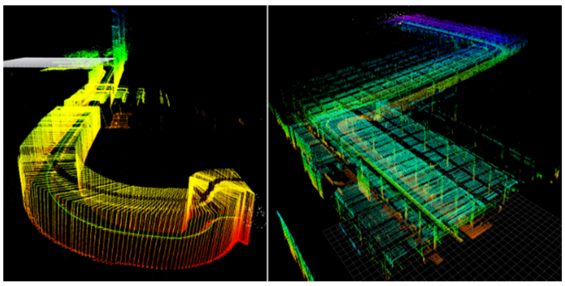

(a) Parking ramp (b) Parking space

Figure 1: Experimental results of the 3D reconstruction for the parking ramp and space by the proposed 3D mapping system.

[a] https://orcid.org/ 0000-0001-5090-9667

Lee, J. and Park, S.
3D Mapping of Indoor Parking Space Using Edge Consistency Census Transform Stereo Odometry.
DOI: 10.5220/0011789100003417
In *Proceedings of the 18th International Joint Conference on Computer Vision, Imaging and Computer Graphics Theory and Applications (VISIGRAPP 2023) - Volume 5: VISAPP*, pages 1015-1020
ISBN: 978-989-758-634-7; ISSN: 2184-4321

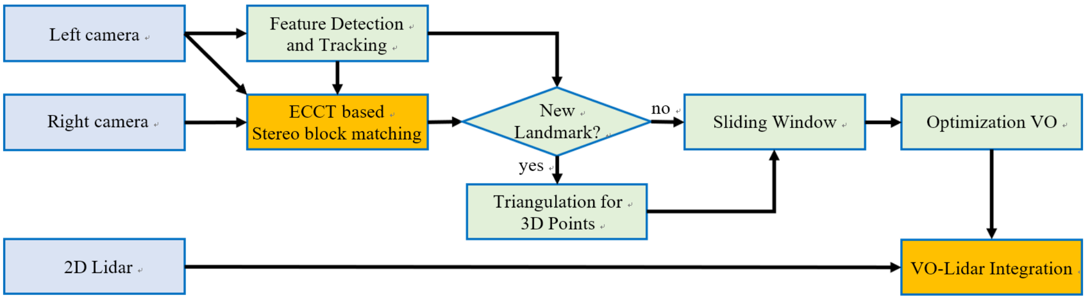

Figure 2: System overview of 3D reconstruction for the parking ramp and parking spaces.

the building law for parking ramp sections suitable for automobile facilities have been established. International building codes include width, height, length, curvature, and slope for ramp sections of buildings. To measure this information, 3D spatial scanning must be accompanied.

In this paper, we propose a 3D mapping system for parking ramps and parking spaces and a mobile mapping device composed of a stereo camera and 2D lidar. The 3D mapping system calculates visual odometry using the proposed ECCT stereo-matching method. The overall system structure of visual odometry is based on VINS-FUSION (Qin et al., 2019). In the parking spaces mapping process, VINS-FUSION's Kanade-Lucas-Tomasi (KLT) stereo matching method causes a large drift error in the vertical direction of the ground (Bouguet, 1999). To reduce this drift error, we estimate the visual odometry using the proposed ECCT stereo matching. ECCT stereo matching is robust to repeated patterns and symmetrical patterns because it considers the continuity and rotation of the edges for the matching block. Next, the point data of the 2D lidar is projected into the 3D space using the 3D coordinate transformation matrix between the stereo camera and the 2D Lidar sensor. Fig. 1 shows the 3D mapping result generated by projecting 2D lidar data into 3D space.

2 SYSTEM OVERVIEW

The proposed 3D mapping device configuration is shown in Fig. 3. The device consists of a stereo camera and 2D lidar, the stereo camera acquires synchronized data through a hardware trigger, and the 2D lidar data acquire synchronized data through software synchronization with the stereo camera. And the system overview of the real-time 3D mapping is shown in Fig. 2. This system takes stereo images as inputs and estimates stereo-based visual odometry (VO). The reference coordinate system of the estimated visual odometry is the left camera coordinate system. In the experiments, we found that VINS-FUSION had a drift problem in the vertical direction of the ground as shown in Fig. 4. VINS-FUSION performs stereo matching based on the KLT feature tracker. We improve the drift problem in the vertical direction of the ground by applying the proposed ECCT stereo matching method. The 2D lidar data is projected onto the 3D space through coordinate system transformation for the estimated VO.

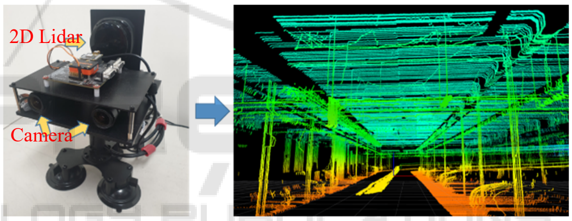

Proposed ing device 3D reconstruction of the parking space

Figure 3: Proposed 3D mapping device for the parking ramp and parking space.

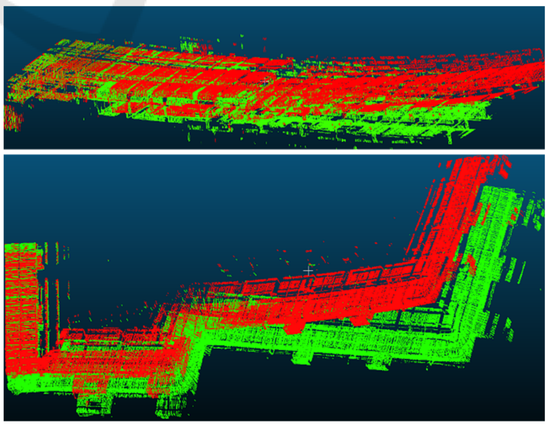

Figure 4: The drift problem with respect to the vertical direction of the ground. The red point cloud is the result of using KLT-based stereo matching. The green point cloud is the result of using the proposed ECCT stereo-matching method.

3 STEREO BLOCK MATCHING

We apply the spare stereo matching method considering real-time applications. A stereo matching point is searched for the tracked feature points between the previous frame and the current frame. The KLT method is used to trace the feature points between the previous frame and the current frame. We propose ECCT stereo-matching for stereo block matching. This method extends the traditional census transform (Zabih and Woodfill, 1994). The proposed method assumes non-rectified stereo images. Rectified stereo images can be easily searched using the epipolar line range search. However, a large part of the image is removed in the process of creating a rectified stereo image. Therefore, the field of view advantage is lost when used in wide-angle images (Lv, 2017). We use a wide-angle camera to take advantage of the wide-angle FOV. We use a window kernel of size (n × n) for stereo matching, where n is an odd value of three or greater. The left image is used as a reference image and the search for stereo matching points in the right image. The search range searches $(w_s \times h_s)$ from the left image to the reference pixel position of the right image. After searching all pixels in the search range, the pixel point with the lowest matching cost value is selected as the stereo matching point. In this paper, n is three and $(w_s \times h_s)$ is (21 × 7).

3.1 Census Transform

Census Transform (CT) creates a binary pattern of 0 and 1 in a window block by comparison between the central pixel and the surrounding pixels. Generates 1 if the center pixel is greater than the neighboring pixel, and 0 if it is less than the neighboring pixel. Then, the matching cost is calculated through the Hamming distance (Liu and Na, 2022) of the generated binary pattern. However, Census Transform Cost (CTC) can produce the same cost results despite different patterns within the search area. This problem often occurs in the repeated pattern (Liu and Collins, 2000) area. Dense stereo matching compensates for this problem mostly in the depth refinement stage (Lee et al., 2012). However, our system must perform spare stereo matching while satisfying real-time performance. Fig. 5 shows an example of the case where the same CTC exists in a size with a window size of 3. If multiple blocks with the same matching cost are found within the search area, matching blocks can be selected in two ways. The first is to randomly select among the same matching cost blocks. The second is to select a matching cost block suitable for the constraint by adding a constraint. We adopt the method of selecting the final matching point by adding a constraint.

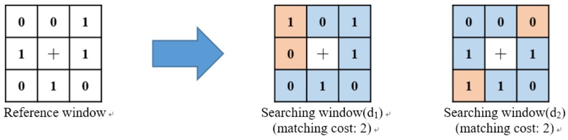

Figure 5: Example of the equal Census Transform cost for different patterns.

3.2 Edge Consistency Census Transform

We propose ECCT stereo-matching to improve CT stereo-matching. We are motivated by fast features (Rosten et al., 2008). The flowchart of the proposed method is shown in Fig. 2. The consistency of the edge area of the binary pattern generated by CT is checked. The edge in the window means the yellow cell in Fig. 6. The order of calculating Edge Consistency Census Transform Cost (ECCTC) is as follows: First, the maximum number of consecutive zeros is searched from the binary bit calculated by CT and defined as the Max count of edge consistency. Assuming that the starting point and the ending point are connected, search for the number of consecutive zeros in clockwise order as shown in Fig. 6. Then, the difference between the total number of edge cells and the max count of edge consistency is calculated. The total number of edge cells (R_{cell}) is defined by (1). Fig. 7 shows an example of calculating ECCTC. In the 1st row of Fig. 7, The max count of edge consistency in the binary bit is 5. And R_{cell} is 8, ECCTC is 8-5=3. Similarly, in the second row of Fig. 7, the max count of edge consistency of binary bits is 2 and ECCTC is 8-2=6. If the consistency of the edge is perfect, the max count of edge consistency is the same as R_{cell}. That is, ECCTC becomes 0. Our final stereo matching cost (T_{cost}) is calculated as the sum of CTC (T_{CT}) and ECCTC (T_{ECCT}) as in (2). The

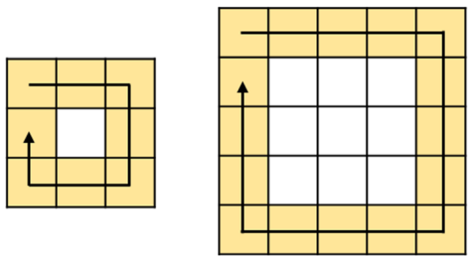

Figure 6: Example of the equal Census Transform cost for different patterns.

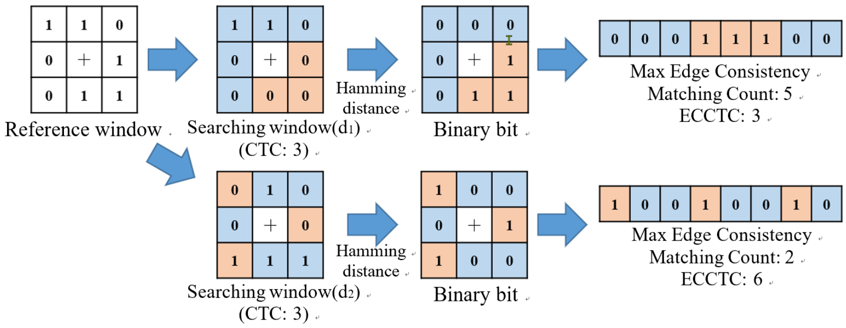

Figure 7: Example of the equal Census Transform cost for different patterns.

proposed ECCT method has an efficient amount of computation because it calculates only the edge part even if the size of the window size increases.

$$R_{cell} = (n-1) * 4 \tag{1}$$

$$T_{cost} = T_{CT} + T_{ECCT} \tag{2}$$

4 VO-LIDAR INTEGRATION

The data from both sensors can be integrated using the coordinate system transformation matrix between the camera and lidar. We project the 2D lidar data onto the visual odometry of the same time. This method can express 3D space using visual odometry and 2D lidar. Equation 3 is a formula for this. $P_L = (x_L, y_L, 1, 1)^T$ represents a point in lidar data measured at time t based on the 2D lidar coordinate system. T_L^C represents the 4x4 transformation matrix between the camera sensor and the 2D lidar sensor. The coordinate system calibration between the two sensors was mechanically corrected. $T_{C_o}^{C_t}$ is the 4x4 transformation matrix of the camera sensor for time t from the world coordinate system. So $P_W = (x_W, y_W, z_W, 1)^T$ is world coordinate data for P_L measured from 2D lidar at time t.

$$P_W = T_{C_o}^{C_t} \times T_L^C \times P_L \tag{3}$$

Figure 8: Mobile Mapping System to acquire data of parking spaces and ramp.

5 EXPERIMENTAL RESULTS

To evaluate the performance of the proposed system, we acquired the dataset from 5 parking ramps and 3 parking spaces by attaching a 3D mapping system to the car as shown in Fig. 8. Each sensor of the proposed 3D scanning device is shown in Table 1. Our camera acquires 20 fps synchronized 688x650 image size data. 2D lidar acquires synchronized data at 10 fps. Computer specs are intel-core i7-9700k @ 3.60 GHz, 16GB RAM.

Table 1: Sensor information of the proposed 3D scanning device.

Type	Manufacture	Model	description
Camera	FILR	GS-U3-41C6C-C	Global shutter camera
Lens	KOWA	LM4NCL	Focal length (3.5mm) Angle of view [Hor×Ver] (117.7° ×86.7°)
2D Lidar	SLAMTech	RPLIDAR S2	1 channel (360 FOV)

We compare the slopes of three parking spaces and present quantitative data for performance comparison between the ECCT stereo matching method and the KLT stereo matching method. Since we do not have exact Ground-Truth (GT) slope information for each parking space, we set two prerequisites. As the first prerequisite, the angle of inclination of the parking spaces is assumed to be zero degrees. As a second prerequisite, we assumed that the normal vector of the plane fitting for the area where the scanned results of the two methods completely overlapped is the normal vector of GT. We calculate the normal vector for two methods of plane fitting and calculate the angle error by calculating the dot product of the GT's normal vector. Table 2 shows the angular error between the normal vector to the ground in GT and the normal vector to

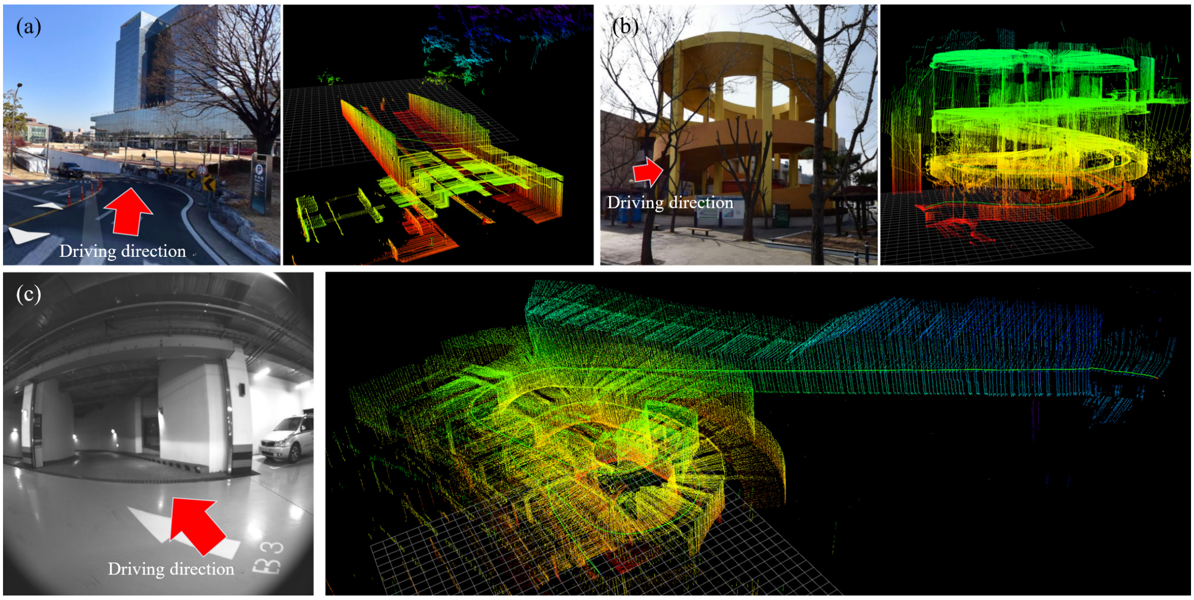

Figure 9: The 3D mapping result for the parking ramps.

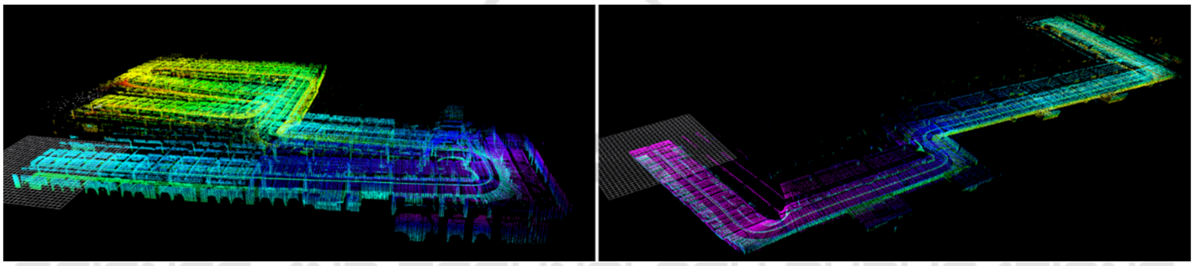

Figure 10: The 3D mapping result for the parking spaces.

the 3D reconstructed point cloud ground. The proposed method shows better performance at the angle error.

Table 2: Angle Error between normal vectors of the ground plane.

	Stereo matching Method	Dataset 1	Dataset 2	Dataset 3
Angle Error (degree)	KLT	7.33994	12.26250	10.19682
	ETTC	1.79957	2.62571	5.33328

Fig. 9 shows the 3D reconstruction results for the three parking ramp section datasets. The left image of each dataset result shows the entry direction of the MMS. The image on the right shows the height ramp map results for the reconstructed point cloud data. Fig. 9(a) is the result of the parking ramp dataset for the scenario going down from the ground floor to the first basement floor. Fig. 9(b) is the result of the parking ramp data set for the scenario going up from the 1st floor to the 4th floor. Fig. 9(c) is the result of the parking ramp data set for the scenario going up from the 3rd basement floor to the 1st floor above the ground. Fig. 10 shows the 3D restoration results for a parking space without a slope.

6 CONCLUSIONS

This paper presents a device consisting of a synchronized stereo camera and a 2D Lidar sensor and the 3D reconstruction method for parking ramp sections and parking spaces in real time. The proposed 3D reconstruction method integrates data by projecting 2D lidar data based on stereo-based visual odometry. Visual odometry is based on VINS-Fusion. The odometry using VINS-Fusion's KLT-based stereo matching can cause drift in the vertical direction to the ground. So, we proposed and integrated the Edge Consistency Census Transform stereo matching method. Edge Consistency Census Transform is designed to be robust against repeated patterns by extending the traditional Census Transform and adding constraints on the consistency of the Census block edge. The proposed method scanned the parking ramp section and parking space and presented qualitative and quantitative results. In future research, we plan to improve the performance of odometry by combining the wheel odometry and an IMU sensor.

ACKNOWLEDGMENT

This work was supported in part by Basic Science Research Program through the National Research Foundation of Korea(NRF) funded by the Ministry of Education (No. 2021R1A6A1A03043144) and part by the NRF grant funded by the Korea government (MSIT)(No. 2021R1A2C2009722).

REFERENCES

Bouguet, J. (1999). Pyramidal implementation of the lucas kanade feature tracker.

Chirca, M., Chapuis, R., & Lenain, R. (2015). Autonomous Valet Parking System Architecture. *2015 IEEE 18th International Conference on Intelligent Transportation Systems*, 2619-2624.

Ding, W., Zhang, L., Chen, J., & Shen, S. (2021). EPSILON: An Efficient Planning System for Automated Vehicles in Highly Interactive Environments. *IEEE Transactions on Robotics, 38*, 1118-1138.

Elhousni, M., Lyu, Y., Zhang, Z., & Huang, X. (2020). Automatic Building and Labeling of HD Maps with Deep Learning. *AAAI Conference on Artificial Intelligence*.

International Code Council, (2018). Overview of the International Building Code, https://codes.iccsafe.org/content/IBC2018.

Kim, K., Cho, S., & Chung, W. (2021). HD Map Update for Autonomous Driving With Crowdsourced Data. *IEEE Robotics and Automation Letters, 6*, 1895-1901.

Lee, S., Park, Y., & Suh, I.H. (2012). Dependable dense stereo matching by both two-layer recurrent process and chaining search. *2012 IEEE/RSJ International Conference on Intelligent Robots and Systems*, 5191-5196.

Liu, P., & Na, J. (2022). A Generalized Hamming Distance of Sequence Patterns.

Liu, Y., & Collins, R.T. (2000). A computational model for repeated pattern perception using frieze and wallpaper groups. *Proceedings IEEE Conference on Computer Vision and Pattern Recognition. CVPR 2000 (Cat. No.PR00662), 1*, 537-544 vol.1.

Lv, Q., Lin, H., Wang, G., Wei, H., & Wang, Y. (2017). ORB-SLAM-based tracing and 3D reconstruction for robot using Kinect 2.0. *2017 29th Chinese Control And Decision Conference (CCDC)*, 3319-3324.

Qin, T., Chen, T., Chen, Y., & Su, Q. (2020). AVP-SLAM: Semantic Visual Mapping and Localization for Autonomous Vehicles in the Parking Lot. *2020 IEEE/RSJ International Conference on Intelligent Robots and Systems (IROS)*, 5939-5945.

Qin, T., Pan, J., Cao, S., & Shen, S. (2019). A General Optimization-based Framework for Local Odometry Estimation with Multiple Sensors. *ArXiv, abs/1901.03638*.

Roh, H.C., Jeong, J., Cho, Y., & Kim, A. (2016). Accurate Mobile Urban Mapping via Digital Map-Based SLAM. *Sensors (Basel, Switzerland), 16*.

Rosten, E., Porter, R.B., & Drummond, T. (2008). Faster and Better: A Machine Learning Approach to Corner Detection. *IEEE Transactions on Pattern Analysis and Machine Intelligence, 32*, 105-119.

Zabih, R., & Woodfill, J.I. (1994). Non-parametric Local Transforms for Computing Visual Correspondence. *European Conference on Computer Vision*.